J. Fluid Mech. (1984), *vol.* 148, *pp.* 247–269
Printed in Great Britain

Motion of a particle generated by chemical gradients. Part 2. Electrolytes

By D. C. PRIEVE, J. L. ANDERSON, J. P. EBEL AND M. E. LOWELL

Department of Chemical Engineering, Carnegie–Mellon University, Pittsburgh, PA 15213

(Received 2 July 1982 and in revised form 7 June 1984)

When immersed in a non-uniform electrolyte solution, a rigid charged sphere migrates toward higher or lower concentration of the electrolyte depending on the relative ionic mobilities and the charge borne by the sphere. This motion has a twofold origin: first, a macroscopic electrolyte gradient produces an electric field which acts on the charged sphere (electrophoresis); secondly, the electrolyte gradient polarizes the cloud of counterions surrounding the charged sphere by making the cloud thinner on the high-concentration side (chemiphoresis). In this paper, we compute the terminal velocity of a non-conductive sphere through a slightly non-uniform solution of a symmetrically charged binary electrolyte. The analysis proceeds through an expansion in the small parameter λ (defined as the ratio of the counterion-cloud thickness to the particle radius). Results to $O(\lambda)$ are presented. The only property of the sphere's surface that affects the velocity is its zeta potential ζ when the electrolyte gradient vanishes; no information concerning the dependence of ζ upon ionic strength is needed. While the chemiphoretic effect always directs the particle toward higher electrolyte concentration, the electrophoretic contribution can move the particle in either direction depending on the sign of $\beta\zeta$, where β is a normalized difference in mobilities between cation and anion of the elecytrolyte; thus particle movement could be directed toward either higher or lower electrolyte concentration depending on the physical properties of the system. With slight algebraic rearrangement, our results are also applicable to conventional electrophoresis (particle motion in an *applied* electric field) and show excellent agreement with the numerical calculations of O'Brien & White (1978).

1. Introduction

When placed in a solution that is macroscopically non-uniform in the concentration of some molecular solute, a colloidal particle moves in response to forces generated by interactions between its surface and the solute molecules. Derjaguin and coworkers (Derjaguin, Dukhin & Korotkova 1961; Dukhin & Derjaguin 1974) introduced the term 'diffusiophoresis' for this motion. In Part 1 of this series (Anderson, Lowell & Prieve 1982) we derived an expression for the velocity of a rigid spherical particle through a viscous fluid containing a macroscopic gradient in the concentration of a non-electrolyte species, when the range of physical interactions between solute molecules and the particle is very short compared with the particle radius. If the interaction between solute molecules and the particle is attractive, the particle migrates toward higher solute concentration, whereas the movement is toward lower solute concentration if the interaction is repulsive.

In this paper we consider a charged spherical particle in a viscous fluid that is macroscopically non-uniform in the concentration of an electrolyte. The action of an electrolyte gradient differs in several respects from that of a non-electrolyte. First, dissolution of a simple salt in water, for example, produces two solute species instead of one: a counterion which is attracted to the charged sphere and a coion which is repelled by the sphere. Secondly, these two ions have different mobilities (diffusion coefficients). In an electrically neutral solution of a symmetrically charged binary electrolyte, equimolar gradients of the concentrations of the two species tend to give rise to cocurrent but unequal diffusion fluxes, and therefore tend to create a 'diffusion current' (Newman 1973). This tendency toward separation of charges is opposed by a macroscopic electric field which arises spontaneously to produce an 'electrical current', equal to the diffusion current but opposite in direction, so that no net current accompanies the diffusion of the salt. Thus, in the simplest case of diffusiophoresis of a charged sphere caused by a gradient in the concentration of a simple salt, there are two species present and a macroscopic electric field, which represent three driving forces for the motion of the sphere.

Derjaguin *et al.* (1961) calculated the migration velocity of a charged sphere in an electrolyte gradient by intuitively extending their analysis for the osmotic flow tangent to an infinite flat plate, generated by a non-electrolyte gradient. Apparently they linearly superimposed the diffusiophoretic velocity, generated by each species acting independently, with the electrophoretic velocity in a macroscopically uniform electrolyte generated by an externally applied field of the same strength as that induced by the salt gradient. Although this approach seems reasonable, few details are given of how the final result was obtained, and no criteria are specified for its validity (except for an infinitesimally thin double layer).

In this paper we seek a solution for the velocity of a charged, rigid, non-conductive sphere spontaneously moving through a slightly non-uniform solution of a binary salt. By 'slightly nonuniform' we mean that, in the absence of the sphere, the change in salt concentration over a distance equal to the radius of the sphere is a small fraction of the salt concentration at the location of the sphere's centre. We confine our attention to conditions for which the thickness of the counterion cloud (i.e. the Debye screening length κ^{-1}) is much smaller than the sphere's radius a. The ion concentration, electrostatic potential and velocity fields are expressed as regular power-series expansions in the small parameter $(\kappa a)^{-1}$, denoted by λ. Separate expansions are obtained inside and outside the counterion cloud, which are then matched to yield the particle velocity $\boldsymbol{u}$ through $O(\lambda)$.

In §2 we obtain $\boldsymbol{u}$ when the counterion cloud is differentially thin ($\lambda = 0$). Profiles inside the cloud are deduced by assuming it to be locally planar and by neglecting any normal flux of ions or fluid. Thus the local fluid velocity immediately outside the cloud is found to be parallel to the local salt gradient. Profiles outside the cloud are obtained by assuming local electroneutrality and by using a boundary condition at the sphere's surface in which slip occurs at a velocity satisfying the inner solution. The resulting velocity field outside the cloud corresponds to potential flow. In the case of a differentially thin cloud, we show that the particle velocity $\boldsymbol{u}$ is independent of the shape as well as the size of the particle, provided that the local mean radius of curvature is everywhere much larger than the Debye length κ^{-1}.

In §3 the mathematical description of the phenomena is reformulated for a spherical particle using a single set of equations, which is uniformly valid both inside and outside the counterion cloud. The solution is obtained in the following form using matched asymptotic expansions:

$$\boldsymbol{u} = \boldsymbol{u}_0 + \lambda \boldsymbol{u}_1 + O(\lambda^2). \tag{1.1}$$

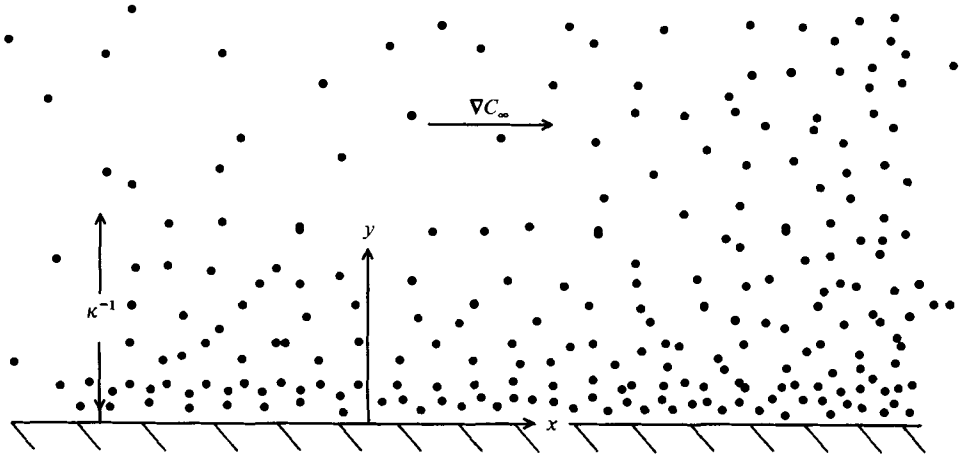

FIGURE 1. Coordinates for flow near an infinite flat plate. κ^{-1} is the Debye screening length. The density of filled circles is meant to represent the concentration of counterions.

In general, $\boldsymbol{u}$ is shown to depend on three independent groups of physical properties: (1) ζ, the zeta potential of the particle in a *uniform* electrolyte solution having the same concentration that the non-uniform solution has at the point where the sphere is immersed; (2) β, the difference between cation and anion mobilities normalized by their sum; and (3) a Péclet number which depends on the charge number and apparent diffusion coefficient for the salt and the temperature, viscosity and dielectric constant of the fluid. The leading term $\boldsymbol{u}_0$ turns out to be identical with that calculated in §2, while $\boldsymbol{u}_1$ is obtained in closed form as multiple integrals, which are evaluated analytically for small ζ and numerically for arbitrary ζ.

Some implications of these results are discussed in §4. Part of the solution for the diffusiophoretic velocity corresponds to the electrophoretic velocity generated by an applied electric field (see Appendix B). That part of the solution is compared to numerical results obtained by O'Brien & White (1978) and an analytical approximation obtained by O'Brien & Hunter (1981). Finally we show that a Padé approximant can be used to extend the results to larger λ.

2. Infinitesimally thin counterion cloud ($\lambda = 0$)

2.1. *Flow near an infinite flat plane*

Consider an interface between a solid with charges affixed to its surface and a binary electrolyte solution which results from the complete dissociation of a simple symmetric salt $\mathrm{M}^{+z}\mathrm{X}^{-z}$ in a polar solvent. Further suppose that this interface forms a plane of infinite area and that the solution resting on this plane is infinitely thick. Let C_+ and C_- denote the local number density of cations and anions respectively, and let the subscript ∞ refer to a distant point in the solution which is beyond the influence of the charged interface. For example, by C_∞ we mean that number density which C_+ and C_- approach as $y \to \infty$ for constant x, where the coordinates x and y are defined in figure 1.

Even when C_∞ is independent of x, as well as y, the charge on the interface gives rise to a nonuniform distribution of ions. Counterions simultaneously experience electrostatic attraction, which tends to bring them to the interface, and Brownian

motion, which tends to distribute them uniformly. If the solution is ideal (i.e. dilute) the flux of either species is given by the Nernst–Planck equation:

$$\boldsymbol{N}_i = -D_i\left[\nabla C_i + \frac{Z_i e C_i}{kT}\nabla\psi\right], \tag{2.1}$$

where $i = +$ and $-$ respectively denote the cation and anion, D_i is the diffusion coefficient of the ion, ψ is the electrostatic potential field, $Z_i e$ is the charge carried by a single ion, k is Boltzmann's constant and T is the absolute temperature. We shall assume $Z_+ = -Z_- = Z$ from here on. At equilibrium, a balance is achieved between the effects of the electrostatic force and Brownian motion such that $\boldsymbol{N}_i = \boldsymbol{0}$ for all x and y, and a Boltzmann distribution of ions arises:

$$C_\pm = C_\infty \exp(\mp\Phi), \tag{2.2}$$

where Φ is the dimensionless electrostatic potential:

$$\Phi = \frac{Ze(\psi - \psi_\infty)}{kT}. \tag{2.3}$$

A second relationship between the distribution of ions and the electrostatic force acting on them is provided by Coulomb's law, which for continua is represented by Poisson's equation:

$$\nabla^2\psi = 4\pi Ze(C_+ - C_-)/\epsilon, \tag{2.4}$$

where ϵ is the dielectric constant of the fluid. Substitution of (2.2) into (2.4) yields the Poisson–Boltzmann equation, which can be integrated (subject to $\psi = \psi_s$ at $y = 0$ and $\psi \to \psi_\infty$ as $y \to \infty$) to obtain

$$\tanh\tfrac{1}{4}\Phi = \gamma\, e^{-\kappa y}, \tag{2.5}$$

where

$$\gamma \equiv \tanh\frac{Ze\zeta}{4kT}, \quad \kappa^2 = \frac{8\pi Z^2 e^2 C_\infty}{\epsilon kT} \tag{2.6), (2.7}$$

and $\zeta = \psi_s - \psi_\infty$. This analysis was first reported by Chapman in 1913. Later, Debye & Hückel solved the linearized form of the Poisson–Boltzmann equation to determine the spherically symmetric distribution of ions about any given central ion as an intermediate step in their theory of thermodynamic activity for strong electrolytes.

The characteristic distance over which Φ (and therefore C_+ and C_-) decays to its asymptotic limit as $y \to \infty$ is called the 'Debye length' κ^{-1}, which varies from about 1 μm in distilled deionized water ($C_\infty \approx 10^{-7}$ M) to about 1 nm in a physiological saline solution ($C_\infty \approx 0.1$ M). The fluid within one or two Debye lengths of a charged interface contains an excess of oppositely charged 'counterions', and hence is not electrically neutral. This layer of solution forming a counterion cloud, together with the layer of fixed charges at the interface, is electrically neutral overall and is collectively called the 'double layer'.

Suppose that C_∞ is not uniform, as was assumed above. In order to have no current arising from cocurrent diffusion of the counterions and coions in an electrically neutral solution, we must require that $\boldsymbol{N}_+ = \boldsymbol{N}_-$ in (2.1), which can only occur if an electric field arises spontaneously:

$$\boldsymbol{E}_\infty = -\nabla\psi_\infty = \frac{kT}{Ze}\beta\nabla\ln C_\infty, \quad \beta = \frac{D_+ - D_-}{D_+ + D_-}. \tag{2.8a,b}$$

This gives rise to a net flux of the electrolyte:

$$\boldsymbol{N}_\infty = -D\nabla C_\infty, \quad D \equiv \frac{2D_+ D_-}{D_+ + D_-}. \tag{2.9a,b}$$

Since $\boldsymbol{N} \neq \boldsymbol{0}$, the solution is not strictly at equilibrium; however, the concentration at nearby points might still be approximately related by Boltzmann's equation. In particular, if the Debye length is much less than the distance over which C_∞ varies appreciably (more precisely, if $|\nabla \ln C_\infty| \ll \kappa$), then ions in the double layer along any normal to the surface are still nearly in equilibrium, so that

$$C_+(x,y) = C_\infty(x) \exp[\mp \Phi(x,y)], \tag{2.10}$$

$$\Phi(x,y) = \frac{Ze}{kT}[\psi(x,y) - \psi_\infty(x)]. \tag{2.11}$$

Furthermore, if the tangential component of the electric field is negligible compared to the normal component (more precisely, if $|\boldsymbol{E}_\infty| \ll \kappa|\zeta|$), then $\partial^2/\partial x^2 \ll \partial^2/\partial y^2$ in (2.4) and integration again yields (2.5)–(2.7), where now $\zeta(x) = \psi(x,0) - \psi_\infty(x)$.

Fluid elements inside the double layer are charged and experience an electrostatic body force. Including this force in Stokes' equation yields

$$-\eta\nabla^2 \boldsymbol{V} + \nabla p + (C_+ - C_-) Ze \nabla\psi = \boldsymbol{0}. \tag{2.12}$$

Scaling arguments applied to the continuity equation show V_x to be the only significant velocity component; thus we may immediately deduce the hydrostatic-pressure profile by integrating the y-component of (2.12) using (2.10) for the ion distributions:

$$p(x,y) - p_\infty = 2kTC_\infty(x)\{\cosh[\Phi(x,y)] - 1\}. \tag{2.13}$$

Substituting this result into the x-component of (2.12) yields

$$\eta\frac{\mathrm{d}^2 V_x}{\mathrm{d}y^2} = (C_+ - C_-) Ze\frac{\mathrm{d}\psi_\infty}{\mathrm{d}x} + 2kT[\cosh\Phi - 1]\frac{\mathrm{d}C_\infty}{\mathrm{d}x}. \tag{2.14}$$

Thus the concentration gradient itself, as well as the electric field induced by the concentration gradient, give rise to an imbalance between the hydrostatic pressure and electrostatic stress. Fluid elements then accelerate until the resulting viscous stress brings the forces into balance. Substituting (2.5) in (2.14), then integrating twice, yields the relative velocity between the distant fluid and the solid:

$$V_x(\infty) - V_x(0) = \frac{\epsilon\zeta}{4\pi\eta}\frac{\mathrm{d}\psi_\infty}{\mathrm{d}x} + \frac{4kT}{\kappa^2\eta}\ln(1-\gamma^2)\frac{\mathrm{d}C_\infty}{\mathrm{d}x}. \tag{2.15}$$

Of course, the first term is just the result obtained by Helmholtz for the relative motion induced by a macroscopic electric field. The second term is an additional contribution which is analogous to motion generated by gradients of non-electrolytes; the form of this term is mathematically equivalent to an expression reported in a footnote by Derjaguin *et al.* (1961). In the absence of an externally applied electric current, $\mathrm{d}\psi_\infty/\mathrm{d}x$ can be deduced from (2.8). After substituting this result together with κ^2 from (2.7), (2.15) becomes

$$V_x(\infty) - V_x(0) = -\frac{\epsilon}{4\pi\eta}\frac{kT}{Ze}\left[\beta\zeta - 2\frac{kT}{Ze}\ln(1-\gamma^2)\right]\frac{\mathrm{d}\ln C_\infty}{\mathrm{d}x}. \tag{2.16}$$

2.2. *Large particles* ($\lambda \to 0$) *of arbitrary shape*

Suppose that the interface portrayed in figure 1 is the surface of a particle of arbitrary shape whose smallest principal radius of curvature $\bar{a}$ at every point on its surface is infinitely greater than the thickness of the counterion cloud ($\kappa\bar{a} \to \infty$). Let $\boldsymbol{x}_0$ be the position of the centre of the particle, and let $\boldsymbol{r} = \boldsymbol{x} - \boldsymbol{x}_0$ be the position in a frame of reference moving with the particle at its velocity $\boldsymbol{U}_0$.†

Consider a closed surface $\mathscr{S}_p^+$ which surrounds the particle and the entire double layer. Since the region enclosed by this surface is electrically neutral, the net force exerted on this boundary by the fluid must vanish (see Appendix A). One solution that satisfies Stokes' equations and this zero-force condition is potential flow:

$$\boldsymbol{V} = -\nabla\phi, \tag{2.17}$$

where, outside of $\mathscr{S}_p^+$, $\phi(\boldsymbol{r})$ satisfies

$$\left.\begin{aligned} \nabla^2\phi &= 0, \\ \boldsymbol{n}\cdot\nabla\phi &= 0 \quad \text{on } \mathscr{S}_p^+, \\ \nabla\phi &\to \boldsymbol{U}_0 \quad (r \to \infty). \end{aligned}\right\} \tag{2.18}$$

Of course $\boldsymbol{U}_0$ is unknown, so (2.17)–(2.18) are incomplete.

Since the fluid is electrically neutral outside the double layer, we have $C_+ = C_- = C$. If convective transport of ions is neglected, then, outside of $\mathscr{S}_p^+$, continuity of the ions and (2.9) reduce to

$$\left.\begin{aligned} \nabla^2 C &= 0, \\ \boldsymbol{n}\cdot\nabla C &= 0 \quad \text{on } \mathscr{S}_p^+, \\ \nabla C &\to \nabla C_\infty = \alpha \boldsymbol{e}_z \quad (r \to \infty), \end{aligned}\right\} \tag{2.19}$$

where $\alpha = |\nabla C_\infty|$. In principle, (2.19) can be solved for $C(\boldsymbol{r})$, but this is not necessary. Note that (2.18) and (2.19) have the same form including the same condition on $\mathscr{S}_p^+$. Now consider the flow within the double layer at the particle surface, which is shown on the scale of κ^{-1} in figure 1. The velocity of the fluid on $\mathscr{S}_p^+$ is found by applying (2.16) with $V_x(0) = 0$, or

$$(\boldsymbol{I} - \boldsymbol{nn})\cdot[\boldsymbol{V} + b\nabla \ln C] = \boldsymbol{0} \quad \text{on } \mathscr{S}_p^+, \tag{2.20}$$

where $-b$ is the coefficient of $\mathrm{d}\ln C_\infty/\mathrm{d}x$ in (2.16).

Although C varies from point to point on $\mathscr{S}_p^+$, the total variation over the entire surface is on the order of αL, where L is a characteristic dimension of the particle. If the undisturbed electrolyte gradient is not too steep, so that $\alpha L \ll C_\infty(\boldsymbol{x}_0)$, then $\nabla \ln C$ in (2.20) can be replaced by $[C_\infty(\boldsymbol{x}_0)]^{-1}\nabla C$. To find $\boldsymbol{U}_0$, we define a function $Y \equiv \phi - [b/C_\infty(\boldsymbol{x}_0)]\, C$, which must satisfy

$$\left.\begin{aligned} \nabla^2 Y &= 0, \\ \nabla Y &= \boldsymbol{0} \quad \text{on } \mathscr{S}_p^+, \\ \nabla Y &\to \boldsymbol{U}_0 - \frac{b}{C_\infty(\boldsymbol{x}_0)}\alpha \boldsymbol{e}_z \quad (r \to \infty). \end{aligned}\right\} \tag{2.21}$$

† The subscript 0 is added here to denote the special case in which $\lambda = 0$.

This problem is ill-posed and has no solution unless $\boldsymbol{U}_0$ takes on that value for which the second boundary condition is $\boldsymbol{\nabla} Y \to \boldsymbol{0}$ as $r \to \infty$. Then the trivial solution ($\boldsymbol{\nabla} Y = \boldsymbol{0}$ for all $\boldsymbol{r}$) is obtained. The particle velocity that admits this solution is

$$\boldsymbol{U}_0 = \frac{\epsilon}{4\pi\eta}\frac{kT}{Ze}\left[\beta\zeta - 2\frac{kT}{Ze}\ln(1-\gamma^2)\right]\boldsymbol{\nabla}\ln C_\infty, \tag{2.22}$$

where $C_\infty(\boldsymbol{x})$ is the electrolyte concentration field in the absence of the particle. This result is generally valid for a particle of any shape in the limit that κ^{-1} is negligibly small compared with the smallest principal radius of curvature at all points on the particle surface. Of course, neglecting convective transport of the electrolyte in (2.19) also requires $U_0 L/D \ll 1$, where D is the electrolyte diffusion coefficient in (2.9). Equation (2.22) was previously deduced by a more intuitive method (Derjaguin *et al.* 1961; Dukhin & Derjaguin 1974).

Morrison (1970) showed that the flow outside the double layer is also irrotational for the motion of a charged particle of arbitrary shape in an applied electric field (electrophoresis), provided that the double layer is everywhere thin compared with the radius of curvature. The problem of diffusiophoresis is similar to electrophoresis in this respect. Again, the irrotational nature of the flow outside the double layer is a consequence of the zero-force constraint discussed in Appendix A and in part 1 of this series. Consequently, the velocity field far from the moving particle decays as r^{-n}, where $n > 1$. Thus the particle cannot be represented by a Stokeslet, but rather is characterized by force dipoles or higher moments. In the case of diffusiophoresis or electrophoresis with $\bar{a} \to \infty$, the velocity is $O(r^{-3})$ rather than $O(r^{-1})$ for Stokes flow, so that hydrodynamic interactions between, say, two particles or one particle and a neighbouring rigid surface will be much weaker. Because the zero-force constraint that leads to this behaviour is characteristic of electrophoresis and diffusiophoresis, we might use the phrase 'phoretic flows' to denote the class of problems that impose this constraint. Not all phoretic flows correspond to potential flow; other velocity fields can also satisfy the zero-force constraint. For example, potential flow is not the outer solution for finite $\kappa\bar{a}$ or when convective transport of the solute is important.

3. Thin counterion cloud ($\lambda \ll 1$)

Although particle size and shape have no effect on diffusiophoretic velocity in the limit $\lambda \to 0$, these geometric factors become important when the Debye length is finite compared with the particle radius. Two considerations must be addressed. First, the distribution of ions cannot be assumed to correspond to thermodynamic equilibrium. Instead one must solve the appropriate convective–diffusion equations inside and outside the double layer. Secondly, the r-component of the fluid velocity near the particle surface is no longer negligibly small, but instead exerts an influence on the distribution of ions within the double layer. As we note below, convection can be significant (when $O(\lambda)$ contributions are considered) even as $Ua/D \to 0$. The notation of § 2 is used in the analysis that follows: in particular, $\boldsymbol{r}$ is the position vector relative to the centre of the moving sphere. The equations describing the ion distributions are solved first, and then the particle velocity is computed to $O(\lambda)$. Fortunately, the coupling between the ion distributions and the fluid velocity occurs at different orders in λ, so that the two sets of equations can still be addressed sequentially.

3.1. *Ion-concentration fields*

The standard convective–diffusion equation with an electrical migration term is used for each ion:

$$\left.\begin{aligned} D_i \nabla\cdot\left[\nabla C_i + \frac{Z_i e}{kT} C_i \nabla\psi\right] &= \boldsymbol{V}\cdot\nabla C_i + \frac{\partial C_i}{\partial t}, \\ \frac{\partial C_i}{\partial r} + \frac{Z_i e}{kT} C_i \frac{\partial\psi}{\partial r} &= 0 \quad (r = a), \\ C_i \to C_\infty(\boldsymbol{x}) = C_\infty(\boldsymbol{x}_0) + \alpha r\cos\theta &\quad (r\to\infty), \end{aligned}\right\} \tag{3.1}$$

where $\boldsymbol{V}$ is the fluid velocity and α is the magnitude of the undisturbed electrolyte gradient. The condition at $r = a$ means that no ions can penetrate or accumulate at the particle surface. As before, we consider only a symmetrically charged electrolyte with $Z = Z_+ = -Z_-$. Changes in the electrical potential are determined from Poisson's equation:

$$\left.\begin{aligned} \nabla^2\psi &= -\frac{4\pi Ze}{\epsilon}[C_+ - C_-], \\ \psi \to \psi_\infty(\boldsymbol{x}) = \psi_\infty(\boldsymbol{x}_0) - \frac{\beta kT\alpha}{ZeC_\infty(\boldsymbol{x}_0)} r\cos\theta &\quad (r\to\infty), \end{aligned}\right\} \tag{3.2}$$

where β is defined by (2.8*b*). We purposely avoid stating the boundary condition on ψ at $r = a$ because, as demonstrated later in this section, it is sufficient to specify the zeta potential, $\zeta = \psi(a) - \psi_\infty(\boldsymbol{x}_0)$, that exists at equilibrium ($\alpha = 0$). In formulating the $r\to\infty$ condition from (2.8), we assume $\alpha a \ll C_\infty(\boldsymbol{x}_0)$ so as to replace $\nabla\ln C_\infty$ by $[C_\infty(\boldsymbol{x}_0)]^{-1}\nabla C_\infty$. Note that subscript ∞ on C and ψ now denotes the 'undisturbed' field that would exist in the absence of the particle.

If the electrolyte solution is only slightly non-uniform, then the perturbations in concentration and potential away from equilibrium (which occurs when $\alpha = 0$) will be small. We define the dimensionless perturbations (c_i^1, Φ^1 and $\boldsymbol{v}^1$) such that

$$C_i = C_i^0 + \alpha a c_i^1 + O(\alpha^2), \tag{3.3a}$$

$$\Phi \equiv \frac{Ze}{kT}[\psi - \psi_\infty(\boldsymbol{x}_0)] = \Phi^0 + \frac{\alpha a}{C_\infty(\boldsymbol{x}_0)}\Phi^1 + O(\alpha^2), \tag{3.3b}$$

$$\boldsymbol{V} = \frac{\alpha kT}{\eta\kappa^2}\boldsymbol{v}^1 + O(\alpha^2), \tag{3.3c}$$

where κ is defined in (2.7). Since $(\mathrm{d}/\mathrm{d}t)\, C_\infty[\boldsymbol{x}_0(t)] = \alpha U$ and since U is $O(\alpha)$, we conclude that $\partial C_i/\partial t$ in (3.1) is $O(\alpha^2)$. In what follows, we neglect all $O(\alpha^2)$ terms. Besides a slightly non-uniform concentration field, this requires that $Ua/D \ll 1$; using (2.7) and substituting the coefficient of $\boldsymbol{v}^1$ in (3.3*c*) for the characteristic speed U, this latter requirement becomes

$$\frac{\alpha a}{C_\infty(\boldsymbol{x}_0)} Pe \ll 1, \tag{3.4}$$

where

$$Pe \equiv \frac{\epsilon}{8\pi\eta D}\left(\frac{kT}{Ze}\right)^2. \tag{3.5}$$

A sample calculation shows that $Pe \approx 0.1$ in aqueous solutions; thus (3.4) is also satisfied if $\alpha a \ll C_\infty(\boldsymbol{x}_0)$. The spatial coordinates are made dimensionless by dividing

them by a ($\rho = r/a$). Substituting (3.3) into (3.1) and (3.2) and collecting terms $O(\alpha^0)$ yields a result that resembles the Boltzmann distribution (2.10):

$$C_+^0 = C_\infty(\boldsymbol{x}_0)\exp(-\Phi^0), \quad C_-^0 = C_\infty(\boldsymbol{x}_0)\exp(+\Phi^0), \tag{3.6a,b}$$

$$\left.\begin{gathered}\frac{1}{\rho^2}\frac{\mathrm{d}}{\mathrm{d}\rho}\left[\rho^2\frac{\mathrm{d}\Phi^0}{\mathrm{d}\rho}\right] = \lambda^{-2}\sinh\Phi^0, \\ \Phi^0 = \bar{\zeta} \equiv \frac{Ze\zeta}{kT} \quad (\rho = 1), \\ \Phi^0 \to 0 \quad (\rho \to \infty),\end{gathered}\right\} \tag{3.6c}$$

where $\lambda = (\kappa a)^{-1}$ is considered a small parameter. The solution for Φ^0 was derived recently by Chew & Sen (1982) as an expansion in λ. In terms of an 'inner variable' $y = \lambda^{-1}(\rho - 1)$ and the surface-charge parameter γ defined in (2.6), their inner expansion is

$$\Phi^0 = \phi_0^0(y) + \lambda\phi_1^0(y) + O(\lambda^2) \quad (y = O(1)), \tag{3.7}$$

$$\phi_1^0 = \frac{2\gamma\,\mathrm{e}^{-y}}{1-\gamma^2\,\mathrm{e}^{-2y}}[\gamma^2(1-\mathrm{e}^{-2y}) - 2y], \tag{3.8}$$

where ϕ_0^0 is given by (2.5). These results are needed later. It is also important to note that, as $\rho \to \infty$, $\Phi^0 \sim \exp[-\lambda^{-1}(\rho-1)]$ for any λ.

The $O(\alpha)$ equations, obtained by substituting (3.3) into (3.1) and (3.2), can be uncoupled and greatly simplified by defining two new variables P and Q:

$$P = (\cos\theta)^{-1}[c_+^1\exp(\Phi^0) + \Phi^1], \tag{3.9a}$$

$$Q = (\cos\theta)^{-1}[c_-^1\exp(-\Phi^0) - \Phi^1], \tag{3.9b}$$

(3.1) then becomes

$$\frac{\mathrm{d}^2P}{\mathrm{d}\rho^2} + \left[\frac{2}{\rho} - \frac{\mathrm{d}\Phi^0}{\mathrm{d}\rho}\right]\frac{\mathrm{d}P}{\mathrm{d}\rho} - \frac{2}{\rho^2}P = (\beta-1)\left[\frac{v_r^1}{\cos\theta}\right]Pe\frac{\mathrm{d}\Phi^0}{\mathrm{d}\rho}, \tag{3.10a}$$

$$\left.\begin{gathered}\frac{\mathrm{d}^2Q}{\mathrm{d}\rho^2} + \left[\frac{2}{\rho} + \frac{\mathrm{d}\Phi^0}{\mathrm{d}\rho}\right]\frac{\mathrm{d}Q}{\mathrm{d}\rho} - \frac{2}{\rho^2}Q = (\beta+1)\left[\frac{v_r^1}{\cos\theta}\right]Pe\frac{\mathrm{d}\Phi^0}{\mathrm{d}\rho}, \\ \frac{\mathrm{d}P}{\mathrm{d}\rho} = \frac{\mathrm{d}Q}{\mathrm{d}\rho} = 0 \quad (\rho = 1), \\ P \to (1-\beta)\rho, \quad Q \to (1+\beta)\rho \quad (\rho \to \infty),\end{gathered}\right\} \tag{3.10b}$$

Besides uncoupling the ion-transport equations, the definitions (3.9) provide another important benefit: they avoid the explicit appearance of Φ^1 in (3.10) or in the boundary conditions; furthermore, the driving force for fluid flow in the double layer (as demonstrated later) is

$$S = (\cos\theta)^{-1}[c_+^1 - c_-^1 + (2\cosh\Phi^0)\Phi^1], \tag{3.11}$$

from which Φ^1 can also be eliminated:

$$S = P\,\mathrm{e}^{-\Phi^0} - Q\,\mathrm{e}^{+\Phi^0}. \tag{3.12}$$

One consequence of eliminating the perturbation in potential is that (to $O(\alpha)$ at least) we do not have to specify how the surface potential is perturbed by the electrolyte gradient: the zeta potential ζ at equilibrium is the only electrostatic property of the particle which affects its diffusiophoretic velocity. The same conclusion was reached by O'Brien & White (1978) in their analysis of electrophoresis.

Our strategy for solving (3.10) is to develop expansions in λ for P and Q in both the inner region ($y = \lambda^{-1}(\rho - 1) = O(1)$) and outer region ($\rho = O(1)$), then to match these expressions appropriately at the boundary of the two regions. To accomplish this, we borrow results from the analysis of the velocity field below, which shows that

$$v_r^1 = [\lambda w_{r,1}(y) + O(\lambda^2)] \cos\theta \quad (y = O(1)) \tag{3.13}$$

with $w_{r,1}(y)$ given by (3.24). After following the above strategy, we obtain the following solution within the inner region:

$$\left.\begin{aligned} P &= P^{(i)} = p_0 + \lambda p_1 + \lambda^2 p_2 + \ldots, \\ Q &= Q^{(i)} = q_0 + \lambda q_1 + \lambda^2 q_2 + \ldots \end{aligned}\right\} \quad (y = O(1)), \tag{3.14}$$

$$p_0 = \tfrac{3}{2}(1-\beta), \quad p_1 = -\left(\frac{1-\beta}{2}\right)\left[3\int_0^\infty (e^{-\Phi^0} - 1)\,dy + Pe\int_0^\infty w_{r,1}\frac{de^{-\Phi^0}}{dy}dy\right],$$

$$q_0 = \tfrac{3}{2}(1+\beta), \quad q_1 = -\left(\frac{1+\beta}{2}\right)\left[3\int_0^\infty (e^{+\Phi^0} - 1)\,dy + Pe\int_0^\infty w_{r,1}\frac{de^{+\Phi^0}}{dy}dy\right].$$

Note that $P^{(i)}$ and $Q^{(i)}$ are independent of y and θ through $O(\lambda)$. A subtle feature of the matching between inner and outer expansions for P and Q is that we had to evaluate the derivative of the $O(\lambda^2)$ term of the inner solution (for example dp_2/dy) in the limit $y \to \infty$ in order to determine p_1 and q_1. The function S is obtained for the inner region by substituting (3.14) into (3.12):

$$S = s_0(y) + \lambda s_1(y) + O(\lambda^2) \quad (y = O(1)), \tag{3.15}$$

$$s_0 = -3[\beta \cosh\phi_0^0 + \sinh\phi_0^0],$$

$$s_1 = -3\phi_1^0[\beta \sinh\phi_0^0 + \cosh\phi_0^0]$$
$$+\frac{3}{2}\left[(1+\beta)e^{\phi_0^0}\int_0^\infty (e^{\phi_0^0(y_1)} - 1)\,dy_1 - (1-\beta)e^{-\phi_0^0}\int_0^\infty (e^{-\phi_0^0(y_1)} - 1)\,dy_1\right]$$
$$+\frac{Pe}{2}\left[(1+\beta)e^{\phi_0^0}\int_0^\infty w_{r,1}(y_1)\frac{de^{\phi_0^0}}{dy_1}dy_1 - (1-\beta)e^{-\phi_0^0}\int_0^\infty w_{r,1}(y_1)\frac{de^{-\phi_0^0}}{dy_1}dy_1\right].$$

ϕ_0^0 and ϕ_1^0 are found in (2.5) and (3.8), while $w_{r,1}$ is given by (3.24).

3.2. *Velocity field*

Stokes' equation is modified to include an electrical body-force term which is non-zero only within the double layer, or when $y = O(1)$. Using dimensional variables,

$$\eta\nabla^2 \boldsymbol{V} - \nabla p - Ze(C_+ - C_-)\nabla\psi = \boldsymbol{0}, \tag{3.16}$$

$$\nabla\cdot\boldsymbol{V} = 0, \tag{3.17}$$

$$\boldsymbol{V} = \boldsymbol{0} \quad (r = a),$$

$$\boldsymbol{V} \to -U\boldsymbol{e}_z + O(r^{-n}) \quad (r \to \infty),$$

where $\boldsymbol{U} = U\boldsymbol{e}_z$ is the particle velocity in a laboratory-fixed reference frame. As discussed in Appendix A, the net force exerted by the fluid on any closed boundary outside the double layer must be zero to $O(\alpha)$, which implies that $\boldsymbol{V}$ decays to $-\boldsymbol{U}$ as $O(r^{-n})$, where $n \geqslant 2$. By requiring $\boldsymbol{V}$ to decay in this manner, the above equations can be solved to obtain U.

After taking the curl of (3.16) and using the dimensionless variables of (3.3) and (3.11), we have the following $O(\alpha)$ terms:

$$\boldsymbol{e}_\phi \cdot \nabla^2(\nabla \times \boldsymbol{v}^1) = \lambda^2 \rho^{-1} S(\rho) \frac{\mathrm{d}\Phi^0}{\mathrm{d}\rho} \sin\theta, \tag{3.18}$$

$$\left.\begin{aligned} \nabla \cdot \boldsymbol{v}^1 &= 0, \\ \boldsymbol{v}^1 &= \boldsymbol{0} \quad (\rho = 1), \\ \boldsymbol{v}^1 &\to -u\boldsymbol{e}_z + O(\rho^{-n}), \quad n \geqslant 2 \quad (\rho \to \infty), \end{aligned}\right\} \tag{3.19}$$

where $\boldsymbol{u}$ is the dimensionless particle velocity,

$$\boldsymbol{u} = \left[\frac{\alpha kT}{\eta\kappa^2}\right]^{-1} \boldsymbol{U}, \tag{3.20}$$

and S is given in general by (3.12) or in the inner region by (3.15). We solve for $\boldsymbol{v}^1$ by considering the inner and outer regions separately and then matching. In the outer region, the right-hand side of (3.18) is $O(\lambda^\infty)$ because $\Phi^0 \sim \exp[-\lambda^{-1}(\rho - 1)]$; thus an outer field that satisfies (3.18)–(3.19) and the $\rho \to \infty$ condition is

$$\boldsymbol{v}^1 = -[u + b\rho^{-3}] \cos\theta\, \boldsymbol{e}_r + [u - b\rho^{-3}] \sin\theta\, \boldsymbol{e}_\theta \quad (\rho = O(1)), \tag{3.21}$$

$$u = u_0 + u_1\lambda + O(\lambda^2), \quad b = b_0 + b_1\lambda + O(\lambda^2).$$

The coefficients u_n and b_n are found by matching this result, expressed in the y-variable, with the inner solution.

In the inner region we expect a solution of the form

$$\boldsymbol{v}^1 = w_r(y) \cos\theta\, \boldsymbol{e}_r + w_\theta(y) \sin\theta\, \boldsymbol{e}_\theta \quad (y = O(1)), \tag{3.22}$$

$$w_r = w_{r,0}(y) + \lambda w_{r,1}(y) + O(\lambda^2),$$

$$w_\theta = w_{\theta,0}(y) + \lambda w_{\theta,1}(y) + O(\lambda^2),$$

$$w_r = w_\theta = 0 \quad (y = 0).$$

The $w_{\theta,n}$ are determined by solving (3.18), one order in λ at a time, with $w_{r,n}$ determined from (3.19). The final equations are

$$\left.\begin{aligned} &\frac{\mathrm{d}w_{r,0}}{\mathrm{d}y} = 0, \quad \frac{\mathrm{d}w_{r,1}}{\mathrm{d}y} = -2w_{\theta,0}, \quad \frac{\mathrm{d}^3 w_{\theta,0}}{\mathrm{d}y^3} = s_0(y) \frac{\mathrm{d}\phi_0^0}{\mathrm{d}y}, \\ &\frac{\mathrm{d}^3 w_{\theta,1}}{\mathrm{d}y^3} = -3\frac{\mathrm{d}^2 w_{\theta,0}}{\mathrm{d}y^2} - y s_0(y) \frac{\mathrm{d}\phi_0^0}{\mathrm{d}y} + s_1(y) \frac{\mathrm{d}\phi_0^0}{\mathrm{d}y} + s_0(y) \frac{\mathrm{d}\phi_1^0}{\mathrm{d}y}. \end{aligned}\right\} \tag{3.23}$$

The solution to these equations is obtained by direct integration, with the integration constants determined from the boundary condition at $y = 0$ and by matching (3.22) with (3.21). $s_n(y)$ and $\phi_n^0(y)$ are found in (3.15), (3.8) and (2.5). Note that $w_{r,1}$ is needed to compute s_1:

$$w_{r,1} = -2\int_0^y \mathrm{d}y_1 \int_0^{y_1} \mathrm{d}y_2 \int_{y_2}^\infty \mathrm{d}y_3 \int_{y_3}^\infty s_0(y_4) \frac{\mathrm{d}\phi_0^0}{\mathrm{d}y_4} \mathrm{d}y_4. \tag{3.24}$$

After matching we obtain

$$u_0 = -b_0 = \frac{1}{3}\int_0^\infty y^2 s_0(y) \frac{\mathrm{d}\phi_0^0}{\mathrm{d}y} \mathrm{d}y, \tag{3.25a}$$

$$u_1 = -b_1 - \frac{1}{3}\int_0^\infty y^3 s_0(y)\frac{\mathrm{d}\phi_0^0}{\mathrm{d}y}\,\mathrm{d}y = -\frac{1}{9}\int_0^\infty y^3 s_0(y)\frac{\mathrm{d}\phi_0^0}{\mathrm{d}y}\,\mathrm{d}y + \frac{1}{3}\int_0^\infty y^2\left[s_1(y)\frac{\mathrm{d}\phi_0^0}{\mathrm{d}y} + s_0(y)\frac{\mathrm{d}\phi_1^0}{\mathrm{d}y}\right]\mathrm{d}y. \quad (3.25b)$$

In dimensional terms, the corresponding particle velocity is

$$\boldsymbol{U} = \frac{\epsilon}{8\pi\eta}\left(\frac{kT}{Ze}\right)^2 [u_0 + u_1\lambda]\,\boldsymbol{\nabla}\ln C_\infty, \quad (3.26)$$

which is correct to $O(\lambda)$.

3.3. *Computation of particle velocity*

After substituting (3.15) for s_0 in (3.25a), using ϕ_0^0 given by (2.5), then integrating, we obtain

$$\left.\begin{aligned} u_0 &= 2\beta\bar{\zeta} - 4\ln(1-\gamma^2), \\ \boldsymbol{U}_0 &= \frac{\epsilon kT'}{4\pi\eta Ze}\left[\beta\zeta - 2\frac{kT}{Ze}\ln(1-\gamma^2)\right]\boldsymbol{\nabla}\ln C_\infty, \end{aligned}\right\} \quad (3.27)$$

where γ is given by (2.6). This result is the same as that derived in §2 using the result of flat-plate analysis as the 'slip velocity'. Unfortunately u_1 cannot in general be expressed in terms of elementary functions of $\bar{\zeta}$. However, if $|\bar{\zeta}|$ is restricted to small values, a regular expansion in powers of $\bar{\zeta}$ can be performed to give

$$u_1 = -6\beta\bar{\zeta} - \tfrac{21}{8}\bar{\zeta}^2 + O(\bar{\zeta}^3). \quad (3.28)$$

Combining this with the $O(\lambda^0)$ result and neglecting $O(\bar{\zeta}^3)$ terms, we obtain

$$\boldsymbol{U} = \frac{\epsilon}{4\pi\eta}\left(\frac{kT}{Ze}\right)^2 [\beta\bar{\zeta}(1-3\lambda) + \tfrac{1}{8}\bar{\zeta}^2(1-\tfrac{21}{2}\lambda)]\,\boldsymbol{\nabla}\ln C_\infty, \quad (3.29)$$

where the error of this expression is $O(\bar{\zeta}^3)$ and $O(\lambda^2)$.

We were forced to numerically evaluate u_1 at larger zeta potentials. A convenient representation of these results which allows substitution of arbitrary β and Pe is

$$u_1 = F_0 + \beta F_1 + Pe[F_2 + \beta(F_3 + F_5) + \beta^2 F_4], \quad (3.30)$$

where the formulae for $F_n(\bar{\zeta})$ are determined by comparing (3.30) with (3.25b) and are given in Appendix B. The asymptotic behaviour of these coefficients as $|\bar{\zeta}| \to 0$ is given by

$$F_0 = -\tfrac{21}{8}\bar{\zeta}^2 + O(\bar{\zeta}^4), \quad F_1 = -6\bar{\zeta} + O(\bar{\zeta}^3), \quad (3.31a,b)$$

$$F_2 = -\tfrac{1}{3}\bar{\zeta}^4 + O(\bar{\zeta}^6), \quad F_3 = -\tfrac{5}{48}\bar{\zeta}^5 + O(\bar{\zeta}^7), \quad (3.31c,d)$$

$$F_4 = -\tfrac{7}{12}\bar{\zeta}^4 + O(\bar{\zeta}^6), \quad F_5 = -2\bar{\zeta}^3 + O(\bar{\zeta}^5). \quad (3.31e,f)$$

Numerical evaluation of these integrals as a function of zeta potential leads to the values shown in table 2 in Appendix B, which are plotted in figures 2 and 3. Except for the requirements that it be binary and symmetric ($Z_+ = -Z_- = Z$), (3.30) is generally applicable to any choice of electrolyte. Physical properties are contained in $\bar{\zeta}$, β and Pe. Note that $F_n(-\bar{\zeta}) = (-1)^n F_n(\bar{\zeta})$.

As a sample calculation, we computed u_0 and u_1 versus zeta potential for three aqueous solutions at 25 °C: NaCl ($\beta = -0.195$, $Pe = 0.16$), KCl ($\beta = -0.0068$, $Pe = 0.13$) and NH_4F ($\beta = 0.147$, $Pe = 0.15$).† These results are plotted in figures 4 and

† These values of β and Pe were computed from (2.8b) and (3.5) using limiting ($C \to 0$) equivalent conductances of the separate ions.

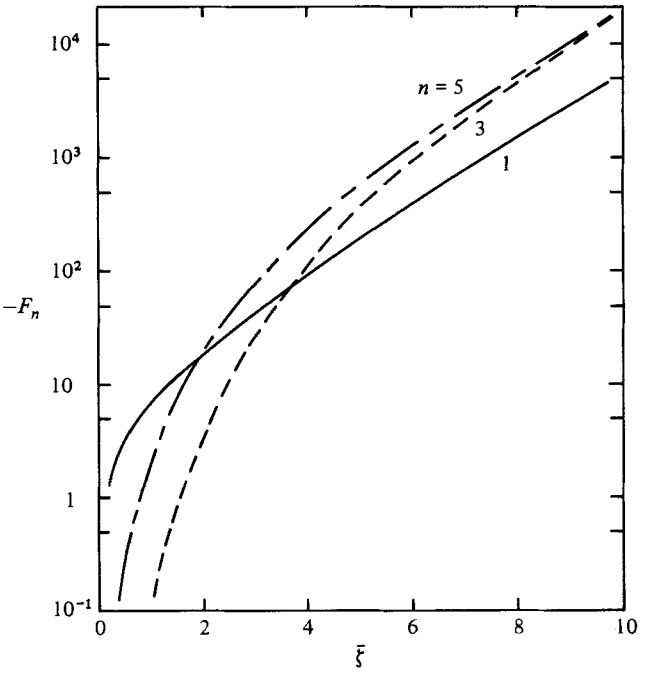

FIGURE 2. Odd functions appearing in (3.30). $\bar{\zeta}$ is the dimensionless zeta potential in the absence of the electrolyte gradient.

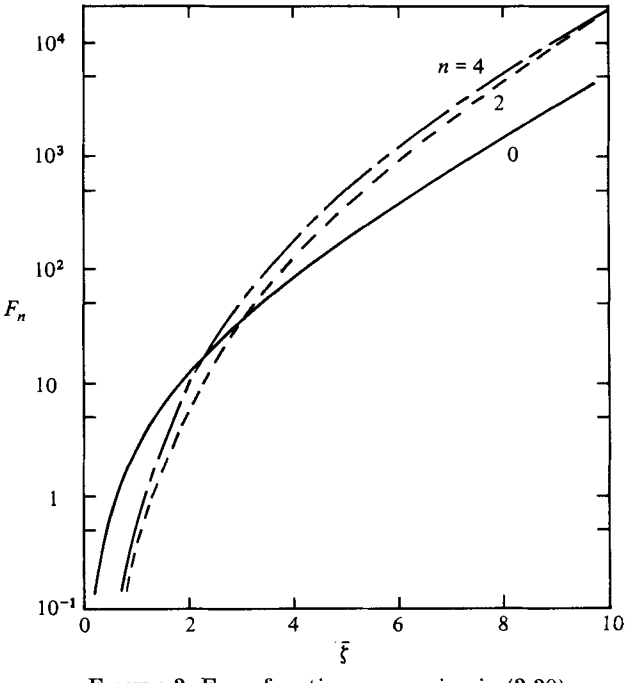

FIGURE 3. Even functions appearing in (3.30).

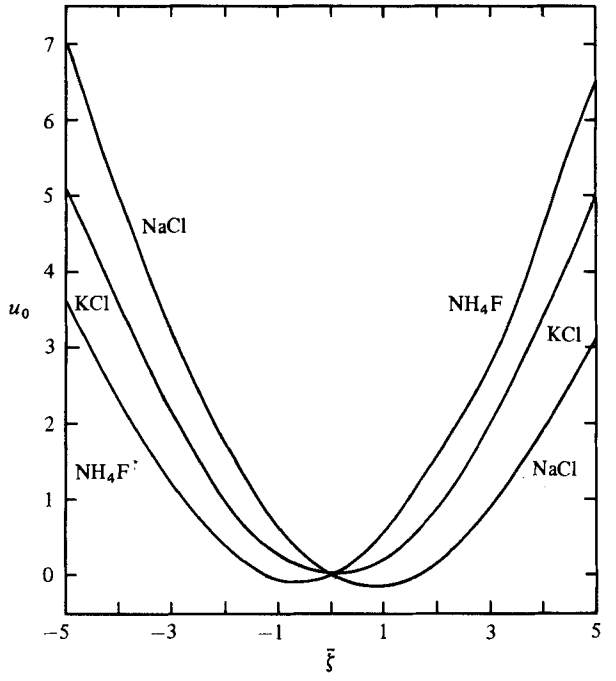

FIGURE 4. Dimensionless $O(\lambda^0)$ contribution to particle velocity (see (3.26)) versus dimensionless zeta potential for three electrolytes in water at 25 °C.

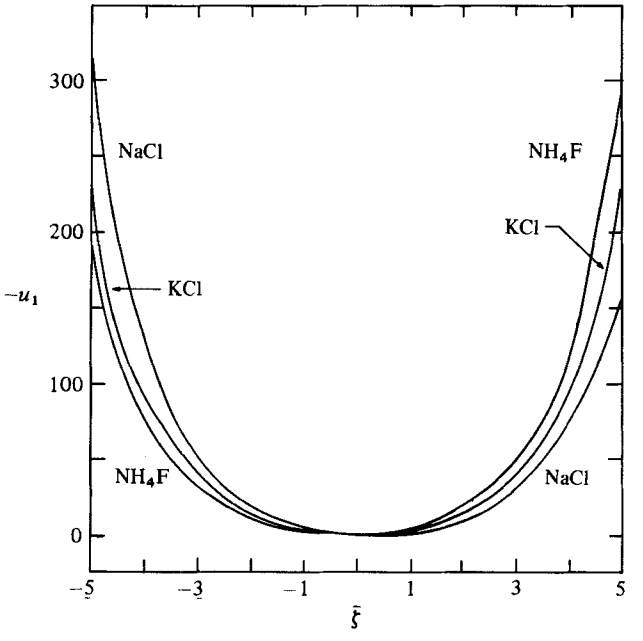

FIGURE 5. Dimensionless $O(\lambda^1)$ contribution to particle velocity (see (3.26)) versus dimensionless zeta potential for three electrolytes in water at 25 °C.

5. Because β is so small for KCl, a charged particle of either sign moves toward higher electrolyte concentration except when $\bar{\zeta}$ is in a small range of positive numbers, for which case the direction is toward lower electrolyte concentration. Because $-\beta$ is larger for NaCl, a particle would move toward lower electrolyte concentration over a broader range of positive zeta potentials.

4. Discussion

Diffusiophoresis can be considered a linear combination of two effects: (1) 'chemiphoresis' due to non-uniform adsorption of counterions over the surface of the sphere, and (2) 'electrophoresis' due to the macroscopic electric field generated by the gradient of electrolyte concentration (see (2.8*a*)):

$$\boldsymbol{U} = \boldsymbol{U}^{(c)} + \boldsymbol{U}^{(e)}, \tag{4.1}$$

$$\boldsymbol{U}^{(c)} = \frac{\epsilon}{8\pi\eta}\left(\frac{kT}{Ze}\right)^2 \{-4\ln(1-\gamma^2) + \lambda[F_0 + Pe(F_2 + \beta F_3)] + O(\lambda^2)\}\nabla \ln C_\infty, \tag{4.2a}$$

$$\boldsymbol{U}^{(e)} = \frac{\epsilon}{8\pi\eta}\frac{kT}{Ze}\{2\bar{\zeta} + \lambda[F_1 + Pe(\beta F_4 + F_5)] + O(\lambda^2)\}\boldsymbol{E}_\infty, \tag{4.2b}$$

where $\bar{\zeta}$ is the dimensionless zeta potential, $\lambda = (\kappa a)^{-1}$, and γ and β are given by (2.6) and (2.8*b*). In appendix C we show that (4.2*b*) also applies to electrophoresis through a macroscopically uniform solution caused by an impressed electric field. The linear superposition in (4.1) is possible because the governing ion-transport equations were linearized with respect to the gradient $\alpha = |\nabla C_\infty|$. If $O(\alpha^2)$ were included, such superposition of the two phenomena would not be possible. Moreover (4.1) and (4.2) apply to solutions in which there are simultaneously an electrolyte concentration gradient and an applied electric field (i.e. current is passed through the solution).

By considering the limit $\lambda \to 0$ and $|\bar{\zeta}| \ll 1$, it is easy to see that chemiphoresis is analogous to diffusiophoresis of non-electrolytes (Anderson *et al.* 1982). For adsorption onto a flat surface, the Gibbs excess concentration of electrolyte at equilibrium is

$$\Gamma = \tfrac{1}{2}\kappa^{-1}\int_0^\infty [C_+ + C_- - 2C_\infty]\,dy = \kappa^{-1}C_\infty\int_0^\infty [\cosh\phi_0^0 - 1]\,dy. \tag{4.3}$$

After substituting ϕ_0^0 from (2.5), we obtain

$$\Gamma = 2\kappa^{-1}C_\infty[\cosh\tfrac{1}{2}\bar{\zeta} - 1],$$

$$\kappa K \equiv \frac{\kappa\Gamma}{C_\infty} = 2[\cosh\tfrac{1}{2}\bar{\zeta} - 1] \to \begin{cases} \tfrac{1}{4}\bar{\zeta}^2 & (\bar{\zeta}\to 0), \\ e^{\frac{1}{2}|\bar{\zeta}|} & (|\bar{\zeta}|\to\infty), \end{cases} \tag{4.4}$$

where K is the 'adsorption length'. For $\lambda = 0$ the chemiphoretic contribution (4.2*a*) can be expressed in terms of K:

$$\boldsymbol{U}_0^{(c)} = \frac{4kT}{\kappa^2\eta}\ln(1 + \tfrac{1}{4}\kappa K)\nabla C_\infty. \tag{4.5}$$

Comparing with the diffusiophoretic velocity for non-electrolytes, given by (4.2) of Anderson *et al.* (1982), we conclude

$$L^*K = 4\kappa^{-2}\ln(1 + \tfrac{1}{4}\kappa K) \to \kappa^{-1}K \quad (K\to 0).$$

Thus, for $\lambda = 0$ and $|\bar{\zeta}| \ll 1$, (4.5) for electrolytes takes on the same form as was previously obtained for non-electrolytes, with the Debye length κ^{-1} corresponding to L^* as well as the length L characterizing the decay of $\Phi(y)$.

For non-electrolytes, Anderson *et al.* concluded that curvature could be neglected if and only if L and K were both much smaller than the particle radius. If this conclusion is applied to electrolytes using $L = \kappa^{-1}$ and (4.4), then

$$\lambda\, e^{\frac{1}{2}|\bar{\zeta}|} \ll 1 \tag{4.6}$$

is sufficient to neglect curvature. Of course, when $|\bar{\zeta}|$ is large, this implies that λ has to be very small indeed, owing to the large value of the adsorption length.

Each term in (4.1) can be expanded separately:

$$\boldsymbol{U}^{(i)} = \boldsymbol{U}_0^{(i)}[1 + G^{(i)}\lambda + O(\lambda^2)], \tag{4.7a}$$

where (i) equals (c) or (e). Since U_1/U_0 may be singular, the total velocity given by (3.26) cannot be expressed in this standard form. Comparing (4.7a) with (4.2) shows that

$$\boldsymbol{U}_0^{(c)} = \frac{\epsilon}{2\pi\eta}\left(\frac{kT}{Ze}\right)^2 [-\ln(1-\gamma^2)]\,\boldsymbol{\nabla} \ln C_\infty, \quad G^{(c)} = -\frac{F_0 + Pe(F_2 + \beta F_3)}{4\ln(1-\gamma^2)}, \tag{4.7b}$$

$$\boldsymbol{U}_0^{(e)} = \frac{\epsilon}{4\pi\eta}\left(\frac{kT}{Ze}\right)^2 \beta\bar{\zeta}\,\boldsymbol{\nabla} \ln C_\infty, \qquad G^{(e)} = (2\bar{\zeta})^{-1}[F_1 + Pe(\beta F_4 + F_5)]. \tag{4.7c}$$

The expression for $\boldsymbol{U}_0^{(e)}$ is equivalent to Smoluchowski's equation for electrophoresis, while our expression for $\boldsymbol{U}_0^{(c)}$ agrees with the expression derived by Anderson (1980) for $|\bar{\zeta}| \ll 1$ and with that presented by Dukhin & Derjaguin (1974) for arbitrary $\bar{\zeta}$. In the case of small zeta potential, (4.7) reduces to (3.29), and hence

$$G^{(c)} = -\tfrac{21}{2} + O(\bar{\zeta}), \quad G^{(e)} = -3 + O(\bar{\zeta}). \tag{4.8a,b}$$

For both chemiphoresis and electrophoresis, curvature retards the speed of the particle. Note that (4.8b) agrees with the $O(\lambda)$ effect derived by Henry (1931) for electrophoresis.

When $|\bar{\zeta}|$ is not small, the coefficients $G^{(i)}$ can become quite large. To neglect $O(\lambda^2)$ in (4.7) we anticipate that a necessary condition is that $|G\lambda| \ll 1$ or that (4.6) is true. Indeed, if $-G^{(c)}\lambda > 1$ and $\beta = 0$, we predict migration toward lower salt concentration, in violation of the second law of thermodynamics. The range of applicability might be expanded by replacing (4.7) with a low-order Padé approximant in which the $O(\lambda^2)$ term is dropped:

$$\boldsymbol{U}^{(i)} = \boldsymbol{U}_0^{(i)}[1 - G^{(i)}\lambda]^{-1}. \tag{4.9}$$

This form avoids sign reversal as λ is increased because the term in brackets is always positive. As shown in table 1, the Padé form for $U^{(e)}$ gives quite good agreement with the 'exact' (numerical) values of O'Brien & White (1978) for electrophoretic mobility. Although we have no exact values of $\boldsymbol{U}^{(c)}$ with which to compare (4.9), we expect good agreement here as well.

A sample calculation illustrates that diffusiophoresis can be an important transport mechanism in boundary layers. Consider a 0.1 μm radius particle having $\bar{\zeta} = -2$ in aqueous NaCl solution having a concentration of 0.1 mol dm^{-3} (M) at 25 °C ($\lambda \approx 10^{-2}$). Let $|\boldsymbol{\nabla} C_\infty| = 1.0$ M cm^{-1}. From (4.7) and table 2 (Appendix B) we have

$$U_0^{(c)} = 0.248\ \mu\text{m/s}, \quad G^{(c)} = -13.7,$$

$$U_0^{(e)} = 0.401\ \mu\text{m/s}, \quad G^{(e)} = -5.32.$$

Substituting these values into (4.9) with $\lambda = 9.6 \times 10^{-3}$ gives

$$U^{(c)} = 0.219\ \mu\text{m/s}, \quad U^{(e)} = 0.381\ \mu\text{m/s}.$$

The diffusive (Brownian-motion) velocity of the particle is D/l, which equals 0.025 μm/s for $l = 100\,\mu$m (a typical boundary-layer thickness). This example

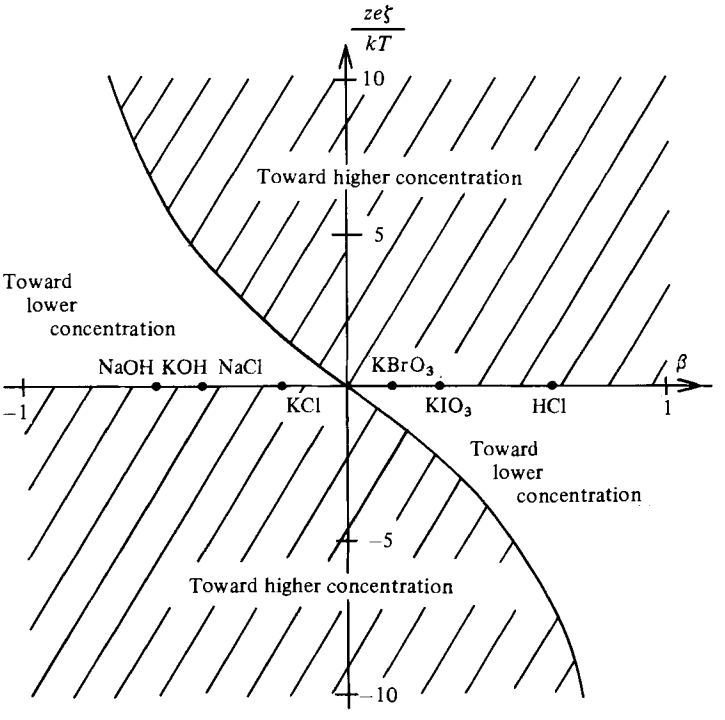

FIGURE 6. A map showing the direction of net migration for $\kappa a = \infty$.

indicates that diffusiophoresis dominates Brownian diffusion and hence would significantly enhance the rate at which particles are transported through the boundary layer. Diffusiophoresis has been used commercially for large-scale coating of metallic surfaces by latex paint (Smith & Prieve 1982).

In the example above, both electrophoresis and chemiphoresis act to move the particle in the direction of higher salt concentration. Generally speaking, chemiphoresis always acts in this direction, while electrophoresis either acts in concert with chemiphoresis or in competition, depending on the sign of $\beta\bar{\zeta}$.

A map showing the direction of net migration is provided in figure 6. Inside the first and third quadrants, chemiphoresis and electrophoresis act in concert to produce migration toward higher salt concentration, while in the second and fourth quadrants the two compete. When competition occurs, a change in the absolute magnitude of $\bar{\zeta}$ can cause a reversal in the direction of migration although the sign of $\bar{\zeta}$ remains the same. This reversal in direction might have some interesting consequences for separating mixtures of similar particles. For example, in a gradient of NaCl, particles having $\bar{\zeta} = 1$ move toward lower concentration, while particles with $\bar{\zeta} = 2$ move in the opposite direction.

This map of directions is for very large particles. For particles of moderate size, the direction of migration also depends on the size. Since a reduction in the radius of curvature tends to retard chemiphoresis more than electrophoresis, the region of the second and fourth quadrants in which electrophoresis wins the competition grows as κa decreases. Let $\bar{\zeta}^*(\beta, Pe, \lambda)$ denote the non-trivial value of $\bar{\zeta}$ for which the two opposing contributions exactly cancel each other to produce $\boldsymbol{U} = \boldsymbol{0}$. For small zeta potentials one can use (4.7) and (4.8) to deduce that

$$\bar{\zeta}^* = -8\,[1 + \tfrac{15}{2}\lambda + O(\lambda^2)]\,\beta \quad (|\bar{\zeta}| \ll 1). \tag{4.10}$$

$\bar{\zeta}$	OW†	(4.12a)	DUK†	OH†
0.3980	0.0310	0.0298	0.0008	0.0052
0.8036	0.0329	0.0320	0.0034	0.0021
1.2267	0.0369	0.0361	0.0080	0.0109
1.6676	0.0432	0.0426	0.0153	0.0220
2.1712	0.0528	0.0528	0.0267	0.0366
2.7340	0.0685	0.0692	0.0445	0.0571
3.4096	0.0940	0.0971	0.0741	0.0885
4.2927	0.1433	0.1502	0.1287	0.1430
5.6640	0.2579	0.2765	0.2519	0.2610
10.000	0.7095	0.7966	0.7143	0.7078

† Numerical values for results of OW, OH and DUK were obtained from tables in O'Brien & Hunter (1981).

TABLE 1. Comparison of various analytical approximations for EM^* at $\lambda = 0.01$ with the numerical results of O'Brien & White (1978)

Thus $\bar{\zeta}^* = \bar{\zeta}^*(\beta, Pe, 0)$ is the equation of the curve in figure 6. Since the value of zeta potential at which a reversal occurs depends on λ, particles of different size but the same zeta potential might migrate in opposite directions.

As a final point of discussion, we remark on the differences between our analysis of the polarized double layer and that of O'Brien & Hunter (1981, hereinafter referred to as OH) which is closely related to the method of Dukhin and coworkers (Dukhin & Derjaguin 1974). OH define the perturbation in double-layer structure by parameters Φ_1 and Φ_2 (see their equation (2.1)), which are related to our perturbation variables when $O(\alpha^2)$ terms are neglected: their Φ_1 is our $-P\cos\theta$, their Φ_2 is our $+Q\cos\theta$, and their equation (3.4) is equivalent to our (3.9). The essential difference is that terms $O(\lambda)$ are neglected in their mathematical solution, but terms $O(\lambda e^{\frac{1}{2}\bar{\zeta}})$ retained; hence the validity of their result is restricted to $\lambda \to 0$ but $e^{\frac{1}{2}\bar{\zeta}}$ sufficiently large that $\lambda e^{\frac{1}{2}\bar{\zeta}}$ is finite (O'Brien 1983).

Although the result of OH shows excellent agreement with the numerical calculations of electrophoretic mobility by O'Brien & White (1978, hereinafter referred to as OW) when $\lambda < 0.02$ and $\bar{\zeta} > 5$, the OH analysis breaks down at smaller $\bar{\zeta}$. Table 1 lists the normalized curvature correction EM^* as a function of $\bar{\zeta}$ for a hypothetical electrolyte ($\approx$ KCl) having $\beta = 0$, $Pe = 0.138$ and $Z = 1$:

$$EM^* \equiv -\frac{EM - \frac{3}{2}\bar{\zeta}}{\frac{3}{2}\bar{\zeta}}, \quad EM = \frac{6\pi\eta Ze}{\epsilon kT}\frac{U^{(e)}}{E_\infty}, \tag{4.11}$$

where E_∞ is the applied electric field. From (4.9) and (2.8a) we have

$$EM^* = \frac{-G^{(e)}\lambda}{1 - G^{(e)}\lambda}, \tag{4.12a}$$

$$\approx \frac{3\lambda}{1+3\lambda} \quad (|\bar{\zeta}| \ll 1), \tag{4.12b}$$

where $G^{(e)}$ is computed from (4.7c). At $\bar{\zeta} \lesssim 1$ we notice that the OH prediction departs significantly from OW, as should be expected since OH did not consistently match inner and outer solutions to $O(\lambda)$. Our result, while not as good as the OH result when $\bar{\zeta}$ is very large, is quite accurate for the entire range of $\lambda < 0.1$ and $|\bar{\zeta}| \lesssim 5$, and is

asymptotically correct as $\lambda \to 0$ at *any* ζ. Note that (4.12*a*) predicts a maximum in EM versus $\bar{\zeta}$ for any given λ, as confirmed by the calculations of OW.

In summary, we have analysed the movement of a charged sphere through a solution having a gradient of concentration of a simple electrolyte. Our perturbation analysis leads to results correct to $O(\lambda)$, as presented in (3.26), (3.27) and (3.30). The required functions $F_n(\bar{\zeta})$ have been computed from the formulas in Appendix B, and the results are numerically displayed there in table 2. To extend the accuracy of the $O(\lambda)$ analysis to larger values of λ, one may use the Padé approximant (4.9) with the expressions in (4.7). Applying this scheme to the electrophoretic component $U^{(e)}$ and comparing the predictions with the calculations of O'Brien & White (1978) for electrophoretic mobility in table 1, we find reasonable agreement for $\lambda \lesssim 0.1$ and $\bar{\zeta} < 10$, and excellent agreement for $\bar{\zeta} < 5$. Given the physical properties $\bar{\zeta} = Ze\zeta/kT$, $\lambda = (\kappa a)^{-1}$, β and Pe (see (2.8*b*) and (3.5) respectively), (4.1), (4.7) and (4.9) can be used to compute particle velocity in an electrolyte gradient with or without an impressed electric current. The major assumption in our analysis is that the electrolyte concentration field is only slightly nonuniform so that the response of the particle is linear in the driving forces; also we have not accounted for asymmetric electrolytes ($Z_+ \neq -Z_-$), weak electrolytes or non-ideal solution behaviour.

This work was supported by a grant from the National Science Foundation and a Fellowship (to J. L. A.) from the John Simon Guggenheim Memorial Foundation.

Appendix A. Velocity far from a charged particle

Consider a surface $\mathscr{S}$ enclosing the particle and surrounding fluid such that $\rho \gg 1$ at all points on $\mathscr{S}$, and let $\boldsymbol{n}$ be the outwardly pointing normal. At steady conditions the total force on the body enclosed by $\mathscr{S}$ must be zero:

$$\int_{\mathscr{S}} \boldsymbol{n}\cdot[\boldsymbol{\tau}_{\mathrm{f}}+\boldsymbol{\tau}_{\mathrm{e}}]\,\mathrm{d}S = \boldsymbol{0}. \tag{A 1}$$

$\boldsymbol{\tau}_{\mathrm{f}}$ is the Newtonian stress tensor, while $\boldsymbol{\tau}_{\mathrm{e}}$ is the Maxwell stress tensor accounting for electrical body forces acting on the body (Woodson & Melcher 1968):

$$\boldsymbol{\tau}_{\mathrm{e}} = \frac{\epsilon}{4\pi}\boldsymbol{E}\boldsymbol{E} - \frac{\epsilon}{8\pi}E^2\boldsymbol{I}, \tag{A 2}$$

where $\boldsymbol{E}$ is the electric field, which is given in terms of the variables in (3.3*b*) as follows:

$$\boldsymbol{E} = -\frac{kT}{Ze}\boldsymbol{\nabla}\left[\Phi^0 + \frac{\alpha a}{C_\infty(\boldsymbol{x}_0)}\Phi^1 + O(\alpha^2)\right]. \tag{A 3}$$

Since $\Phi^0 \sim \exp(-\lambda^{-1}\rho) \to 0$ and $|\boldsymbol{\nabla}\Phi^1| \sim \beta$ as $\rho \to \infty$,

$$\boldsymbol{\tau}_{\mathrm{e}} \to O(\alpha^2) \quad \text{as} \quad \rho \to \infty. \tag{A 4}$$

From (A 1) we have

$$\lim_{\rho\to\infty} \int_{\mathscr{S}} \boldsymbol{n}\cdot\boldsymbol{\tau}_{\mathrm{f}}\,\mathrm{d}S = O(\alpha^2), \tag{A 5}$$

and hence the net fluid (viscous) stress on $\mathscr{S}$ is zero to $O(\alpha)$.

Far outside the double layer ($\rho - 1 \gg \lambda$) the axisymmetric flow field is governed

by the homogeneous Stokes equations, whose stream function has the following general form:

$$\Psi(\rho,\theta) = \sum_{n=2}^{\infty} [A_n \rho^n + B_n \rho^{-n+3} + C_n \rho^{-n+1}] I_n(\cos\theta), \tag{A 6}$$

where the I_n are Gegenbauer functions of the first kind, and A_2 equals $\frac{1}{2}U$ while $A_n = 0$ for $n \geqslant 3$. Using (A 6) one has (Happel & Brenner 1973)

$$\int_{\mathscr{S}} \boldsymbol{n}\cdot\boldsymbol{\tau}_{\mathrm{f}}\,\mathrm{d}S = \frac{4\pi}{a}\eta B_2 \boldsymbol{e}_z. \tag{A 7}$$

Comparing (A 5) with (A 7), we have $B_2 = O(\alpha^2)$, so that to $O(\alpha)$ the far-field velocity must decay to $-\boldsymbol{U}$ as ρ^{-n}, where $n \geqslant 2$.

Appendix B. Evaluation of $F_n(\zeta)$ in (3.30)

The six coefficients in (3.30) were determined to be the following:

$$F_0(\bar{\zeta}) = \frac{1}{3}\int_0^{\infty}\left[y^3 \sinh\phi_0^0 \frac{\mathrm{d}\phi_0^0}{\mathrm{d}y} - 3y^2 \sinh\phi_0^0 \frac{\mathrm{d}\phi_1^0}{\mathrm{d}y} + y^2 f_0 \frac{\mathrm{d}\phi_0^0}{\mathrm{d}y}\right]\mathrm{d}y, \tag{B 1}$$

$$F_1(\bar{\zeta}) = \frac{1}{3}\int_0^{\infty}\left[y^3 \cosh\phi_0^0 \frac{\mathrm{d}\phi_0^0}{\mathrm{d}y} - 3y^2 \cosh\phi_0^0 \frac{\mathrm{d}\phi_1^0}{\mathrm{d}y} + y^2 f_1 \frac{\mathrm{d}\phi_0^0}{\mathrm{d}y}\right]\mathrm{d}y, \tag{B 2}$$

$$F_n(\bar{\zeta}) = \frac{1}{3}\int_0^{\infty} y^2 f_n \frac{\mathrm{d}\phi_0^0}{\mathrm{d}y}\mathrm{d}y \quad (n = 2, \ldots, 5), \tag{B 3}$$

where

$$f_0(y) = -3\phi_1^0 \cosh\phi_0^0 + \frac{3}{2}\left[\mathrm{e}^{\phi_0^0}\int_0^{\infty}(\mathrm{e}^{\phi_0^0(y_1)} - 1)\,\mathrm{d}y_1 - \mathrm{e}^{-\phi_0^0}\int_0^{\infty}(\mathrm{e}^{-\phi_0^0(y_1)} - 1)\,\mathrm{d}y_1\right] \tag{B 4a}$$

$$= -3\phi_1^0 \cosh\phi_0^0 + 6[\sinh(\tfrac{1}{2}\bar{\zeta})\cosh\phi_0^0 + \cosh(\tfrac{1}{2}\bar{\zeta})\sinh\phi_0^0 - \sinh\phi_0^0], \tag{B 4b}$$

$$f_1(y) = -3\phi_1^0 \sinh\phi_0^0 + \frac{3}{2}\left[\mathrm{e}^{\phi_0^0}\int_0^{\infty}(\mathrm{e}^{\phi_0^0(y_1)} - 1)\,\mathrm{d}y_1 + \mathrm{e}^{-\phi_0^0}\int_0^{\infty}(\mathrm{e}^{-\phi_0^0(y_1)} - 1)\,\mathrm{d}y_1\right] \tag{B 5a}$$

$$= -3\phi_1^0 \sinh\phi_0^0 + 6[\sinh(\tfrac{1}{2}\bar{\zeta})\sinh\phi_0^0 + \cosh(\tfrac{1}{2}\bar{\zeta})\cosh\phi_0^0 - \cosh\phi_0^0], \tag{B 5b}$$

$$f_2(y) = \frac{1}{2}\left[\mathrm{e}^{\phi_0^0}\int_0^{\infty} I_0(y_1)\frac{\mathrm{d}\,\mathrm{e}^{\phi_0^0}}{\mathrm{d}y_1}\mathrm{d}y_1 - \mathrm{e}^{-\phi_0^0}\int_0^{\infty} I_0(y_1)\frac{\mathrm{d}\,\mathrm{e}^{-\phi_0^0}}{\mathrm{d}y_1}\mathrm{d}y_1\right] \tag{B 6a}$$

$$= -\mathrm{e}^{\phi_0^0}\int_0^{\infty} I_0(y_1)\,\mathrm{e}^{\phi_0^0(y_1)}\sinh[\tfrac{1}{2}\phi_0^0(y_1)]\,\mathrm{d}y_1 - e^{-\phi_0^0}\int_0^{\infty} I_0(y_1)\,\mathrm{e}^{-\phi_0^0(y_1)}\sinh[\tfrac{1}{2}\phi_0^0(y_1)]\,\mathrm{d}y_1, \tag{B 6b}$$

$$f_3(y) = \frac{1}{2}\left[\mathrm{e}^{\phi_0^0}\int_0^{\infty} I_0(y_1)\frac{\mathrm{d}\,\mathrm{e}^{\phi_0^0}}{\mathrm{d}y_1}\mathrm{d}y_1 + \mathrm{e}^{-\phi_0^0}\int_0^{\infty} I_0(y_1)\frac{\mathrm{d}\mathrm{e}^{-\phi_0^0}}{\mathrm{d}y_1}\mathrm{d}y_1\right] \tag{B 7a}$$

$$= -\mathrm{e}^{\phi_0^0}\int_0^{\infty} I_0(y_1)\,\mathrm{e}^{\phi_0^0(y_1)}\sinh[\tfrac{1}{2}\phi_0^0(y_1)]\,\mathrm{d}y_1 + e^{-\phi_0^0}\int_0^{\infty} I_0(y_1)\,\mathrm{e}^{-\phi_0^0(y_1)}\sinh[\tfrac{1}{2}\phi_0^0(y_1)]\,\mathrm{d}y_1, \tag{B 7b}$$

$$f_4(y) = \frac{1}{2}\left[\mathrm{e}^{\phi_0^0}\int_0^{\infty} I_1(y_1)\frac{\mathrm{d}\mathrm{e}^{\phi_0^0}}{\mathrm{d}y_1}\mathrm{d}y_1 + \mathrm{e}^{-\phi_0^0}\int_0^{\infty} I_1(y_1)\frac{\mathrm{d}\,\mathrm{e}^{-\phi_0^0}}{\mathrm{d}y_1}\mathrm{d}y_1\right] \tag{B 8a}$$

$$= -\mathrm{e}^{\phi_0^0}\int_0^{\infty} I_1(y_1)\,\mathrm{e}^{\phi_0^0(y_1)}\sinh[\tfrac{1}{2}\phi_0^0(y_1)]\,\mathrm{d}y_1 + \mathrm{e}^{-\phi_0^0}\int_0^{\infty} I_1(y_1)\,\mathrm{e}^{-\phi_0^0(y_1)}\sinh[\tfrac{1}{2}\phi_0^0(y_1)]\,\mathrm{d}y_1, \tag{B 8b}$$

$$f_5(y) = \frac{1}{2}\left[e^{\phi_0^0} \int_0^\infty I_1(y_1) \frac{d e^{\phi_0^0}}{dy_1} dy_1 - e^{-\phi_0^0} \int_0^\infty I_1(y_1) \frac{d e^{-\phi_0^0}}{dy_1} dy_1 \right] \tag{B 9a}$$

$$= -e^{\phi_0^0} \int_0^\infty I_1(y_1)\, e^{\phi_0^0(y_1)} \sinh\left[\tfrac{1}{2}\phi_0^0(y_1)\right] dy_1 - e^{-\phi_0^0} \int_0^\infty I_1(y_1)\, e^{-\phi_0^0(y_1)} \sinh\left[\tfrac{1}{2}\phi_0^0(y_1)\right] dy_1, \tag{B 9b}$$

$$I_0(y) = 6 \int_0^y dy_1 \int_0^{y_1} dy_2 \int_{y_2}^\infty dy_3 \int_{y_3}^\infty \sinh\left(\phi_0^0(y_4)\right) \frac{d\phi_0^0}{dy_4} dy_4 \tag{B 10a}$$

$$= 12\left[y \ln(1-\gamma^2) - \int_0^y \ln\left(1-\gamma^2 e^{-2y_1}\right) dy_1 \right], \tag{B 10b}$$

$$I_1(y) = 6 \int_0^y dy_1 \int_0^{y_1} dy_2 \int_{y_2}^\infty dy_3 \int_{y_3}^\infty \cosh\left(\phi_0^0(y_4)\right) \frac{d\phi_0^0}{dy_4} dy_4 \tag{B 11a}$$

$$= -24\left[y \tanh^{-1}\gamma + \int_0^y \tanh^{-1}\left(\gamma e^{-y_1}\right) dy_1 \right]. \tag{B 11b}$$

The second equation of each pair above was obtained by substituting (2.5) for $\phi_0^0(y)$ and (3.8) for $\phi_1^0(y)$. Numerical values of the six coefficients are tabulated in table 2 for some positive values of $\bar{\zeta}$. Corresponding values of the coefficients for negative $\bar{\zeta}$ can be deduced from

$$F_n(-\bar{\zeta}) = (-1)^n F_n(\bar{\zeta}) \quad (n = 0, 1, \ldots, 5). \tag{B 12}$$

Appendix C. Electrophoresis of a rigid sphere

In electrophoresis the particle movement is driven by an applied electric field ($\boldsymbol{E}_\infty = E_\infty \boldsymbol{e}_z$), and the undisturbed electrolyte concentration is constant (C_∞). Equations (3.1) and (3.2) still apply, except that the far-field boundary condition is altered:

$$\left.\begin{aligned} &C_+ \to C_- \to C_\infty, \\ &\psi \to \psi_\infty(\boldsymbol{x}_0) - E_\infty r\cos\theta \end{aligned}\right\} \quad (r \to \infty). \tag{C 1}$$

The following replace (3.3):

$$\left.\begin{aligned} C_i &= C_i^0 + \mu a C_\infty c_i^1 + O(\mu^2), \\ \boldsymbol{\Phi} &= \boldsymbol{\Phi}^0 + \mu a \boldsymbol{\Phi}^1 + O(\mu^2), \\ \boldsymbol{V} &= \frac{\mu C_\infty kT}{\eta\kappa^2} \boldsymbol{v}^1 + O(\mu^2), \end{aligned}\right\} \tag{C 2}$$

where $\mu = (Ze/kT)\, E_\infty$. Substituting (C 2) into (3.1) and (3.2) and collecting $O(\mu^0)$ terms yields (3.6), while the $O(\mu^1)$ terms give (3.10) with the following far-field boundary conditions:

$$P \to -\rho, \quad Q \to +\rho \quad (\rho \to \infty).$$

The solution for P and Q to $O(\lambda)$ in the inner region is

$$\left.\begin{aligned} p_0 &= -\tfrac{3}{2}, \quad q_0 = \tfrac{3}{2}, \\ p_1 &= \frac{3}{2}\int_0^\infty (e^{-\phi_0^0} - 1)\, dy - \tfrac{1}{2}(1-\beta)\, Pe \int_0^\infty w_{r,1} \frac{d e^{-\phi_0^0}}{dy} dy, \\ q_1 &= -\frac{3}{2}\int_0^\infty (e^{\phi_0^0} - 1)\, dy - \tfrac{1}{2}(1+\beta)\, Pe \int_0^\infty w_{r,1} \frac{d e^{\phi_0^0}}{dy} dy, \end{aligned}\right\} \tag{C 3}$$

$\bar{\zeta}$	$-F_0$	$-F_1$	$-F_2$	$-F_3$	$-F_4$	$-F_5$
0.0000	0.0000	0.0000	0.0000	0.0000	0.0000	0.0000
0.2503	0.16498	1.5124	0.0013117	0.00010238	0.0022920	0.031452
0.3980	0.41897	2.4302	0.0084115	0.0010404	0.014664	0.12692
0.8036	1.7482	5.1742	0.14222	0.034929	0.24510	1.0659
1.0000	2.7529	6.6865	0.34526	0.10427	0.59016	2.0838
1.2267	4.2424	8.6460	0.79535	0.28979	1.3443	3.9252
1.6776	8.4338	13.480	2.9041	1.3887	4.7748	10.567
2.0000	12.657	17.980	6.0878	3.3507	9.7812	18.725
2.1712	15.406	20.830	8.6398	5.0589	13.701	24.597
2.4385	20.533	26.063	14.250	9.0624	22.120	36.426
2.7340	27.598	33.188	23.500	16.111	35.597	54.149
3.0000	35.475	41.081	35.484	25.730	52.559	75.317
3.3716	49.460	55.044	60.102	46.445	86.273	115.44
3.4096	51.120	56.699	63.258	49.164	90.515	120.37
4.000	83.705	89.185	132.63	110.90	180.80	221.94
4.2927	105.71	111.13	185.423	159.35	247.03	294.13
5.0000	181.63	186.89	389.37	351.59	492.83	555.03
5.6440	295.01	300.14	729.66	679.62	885.44	962.40
6.000	374.50	379.56	982.81	926.21	1170.1	1254.7
6.7801	642.13	647.08	1882.9	1810.4	2157.1	2259.5
7.0000	745.07	749.99	2241.5	2164.3	2543.7	2651.2
8.0000	1443.0	1447.8	4762.5	4664.0	5212.0	5342.4
9.0000	2736.8	2741.6	9619.5	9499.0	10249	10402
10.000	5105.5	5110.2	18727	18585	19569	19745

TABLE 2. Numerical values of $F_n(\bar{\zeta})$ in (3.30)

where $w_{r,1}$ is given by (3.24). After substituting (C 3) into (3.12) and expanding according to (3.15), we have

$$s_0 = -3\cosh\phi_0^0 \quad s_1 = f_1(y) + \beta Pe f_4(y) + Pe f_5(y), \tag{C 4}$$

where the f_n are found in Appendix B. Using this result in (3.25) gives, in dimensional form, the electrophoretic velocity:

$$\boldsymbol{U} = \frac{\epsilon}{8\pi\eta}\frac{kT}{Ze}(u_0 + \lambda u_1)\boldsymbol{E}_\infty, \tag{C 5}$$

$$u_0 = 2\bar{\zeta}, \quad u_1 = F_1 + Pe(\beta F_4 + F_5), \tag{C 6}$$

which is asymptotically correct to $O(\lambda)$. Note that the $O(\lambda^0)$ result is Smoluchowski's expression.

REFERENCES

ANDERSON, J. L. 1980 Motion of a charged particle in a gradient of electrolyte. *Physicochem. Hydrodyn.* **1**, 51.

ANDERSON, J. L., LOWELL, M. E. & PRIEVE, D. C. 1982 Motion of a particle generated by chemical gradients. Part I. Non-electrolytes. *J. Fluid Mech.* **117**, 107.

CHEW, W. C. & SEN, P. N. 1982 Potential of a sphere in an ionic solution in thin double layer approximations. *J. Chem. Phys.* **77**, 2042.

DERJAGUIN, B. V., DUKHIN, S. S. & KOROTKOVA, A. A. 1961 Diffusiophoresis in electrolyte solutions and its role in the mechanism of film formation from rubber latexes by the method of ionic deposition. *Kolloidn. Zh.* **23**, 53.

DUKHIN, S. S. & DERJAGUIN, B. V. 1974 Electrokinetic phenomena. In *Surface and Colloid Science* (ed. E. Matijevic), vol. 7. Wiley.

HAPPEL, J. & BRENNER, H. 1973 *Low Reynolds Number Hydrodynamics.* Noordhoff.

HENRY, D. C. 1931 The cataphoresis of suspended particles. Part 1. The equation of cataphoresis. *Proc. R. Soc. Lond.* A **133**, 106.

MORRISON, F. A. 1970 Electrophoresis of a particle of arbitrary shape. *J. Colloid Interface Sci.* **34**, 210.

NEWMAN, J. S. 1973 *Electrochemical Systems.* Prentice-Hall.

O'BRIEN, R. W. 1983 The solution of the electrokinetic equations for colloidal particles with thin double layers. *J. Colloid Interface Sci.* **92**, 204.

O'BRIEN, R. W. & HUNTER, R. J. 1981 The electrophoretic mobility of large colloidal particles. *Can. J. Chem.* **59**, 1878.

O'BRIEN, R. W. & WHITE, L. R. 1978 Electrophoretic mobility of a spherical colloidal particle. *J. Chem. Soc. Faraday Trans. II* **72**, 1607.

SMITH, R. E. & PRIEVE, D. C. 1982 Accelerated deposition of latex particles onto a rapidly dissolving steel surface. *Chem. Engng Sci.* **37**, 1213.

WOODSON, H. H. & MELCHER, J. R. 1968 *Electromechanical Dynamics* (*Part II*). Wiley.